RSC Advances

PAPER

View Article Online
View Journal | View Issue

Cite this: *RSC Adv.*, 2021, **11**, 26102

Optimizing the composition of LiFSI-based electrolytes by a method combining simplex with normalization

Hongli Lu,[ab] Shuangwei Zeng,[ab] Dongni Zhao,[ab] Jie Wang,[ab] Yin Quan,[ab] Fei Xu,[ab] Faqiang Li[c] and Shiyou Li *[ab]

The optimizing method of electrolyte formulation is always vital for the development of high-performance lithium-ion batteries. Traditional optimization methods are mainly aimed at the optimization of the electrolyte composition type, and less attention is paid to the optimization of the composition proportion in a certain electrolyte formulation. In this paper, in order to balance the relationship between aluminum (Al) foil corrosion inhibition and battery electrochemical performance, the electrolyte system $LiFSI_{0.6}$–$LiBOB_{0.4}$–EC/DEC/EMC (1 : 1 : 1, by volume) was optimized by combining the simplex method, normalization and electrochemical testing. A lithium iron phosphate ($LiFePO_4$) cathode with the optimized electrolyte of $LiFSI_{0.53}$–$LiBOB_{0.35}$–EC/DEC/EMC (1.3 : 1.5 : 1.5) delivers a high capacity (143.1 mA h g^{-1} at 0.5C) and remarkable cycle life (94.9% retention after 100 cycles) at 45 °C. The outstanding performance is attributed to the composition of the cathode electrolyte interphase (CEI) containing the solid and dense LiF, AlF_3, B_2O_3 and Li_2CO_3. This provides a new method and idea for future electrolyte formulation optimization.

Received 4th July 2021
Accepted 20th July 2021

DOI: 10.1039/d1ra05156c

rsc.li/rsc-advances

1. Introduction

Lithium-ion batteries (LIBs) have been widely used in the field of electric vehicles due to the electrochemical energy storage devices with safety and high efficiency.[1] Nevertheless, there are a few problems in LIBs. Firstly, the dominant lithium salt in commercial electrolyte, lithium hexafluorophosphate ($LiPF_6$), cannot meet the requirements of high-power energy storage, because of the poor thermal stability and strong hydrolysis ability,[2,3] although the thermal decomposition products counteract thermal runaway and can scavenge dissolved transition metals and prevent crosstalk and rollover failure.[4,5] Secondly, the battery arrangement is very compact in order to save space, which makes it difficult to release the heat and results in the failure of batteries. Therefore, finding a high-performance electrolyte suitable for extreme conditions is urgent to be solved. Nowadays, it is necessary to optimize the $LiPF_6$-based electrolyte system or find alternatives. Lithium bis(fluorosulfonyl)imide (LiFSI) has attracted attention because of its excellent thermal stability and high solubility.[6–9] However, the corrosion of the Al current collector limits its application in LIBs.[10] To solve this problem, lithium difluoro(oxalato)borate (LiDFOB), lithium tetrafluoroborate ($LiBF_4$) and $LiPF_6$ additives are added into LiFSI-based electrolyte for suppressing corrosion.[11–14] Among these electrolytes containing additives, an Al current collector is stable up to 5.0 V (*vs.* Li/Li^+) in organic electrolytes containing LiBOB since an effective passivation layer can be formed on the Al surface.[15,16] The previous work has showed that research on a LiFSI-based nonaqueous electrolyte, $LiFSI_{0.6}$–$LiBOB_{0.4}$–EC/DEC/EMC (1 : 1 : 1), was successfully applied for suppressing Al corrosion caused by LiFSI at 45 °C.[17] The electrolyte can effectively inhibit the Al corrosion, caused by the dissolution of co-generated $Al(FSI)_3$. The result is attributed to that the interfacial film with the boron-containing compounds can promote the change from AlF_3 to LiF and reinforce the interphase stability. However, for the electrolyte system of $LiFSI_{0.6}$–$LiBOB_{0.4}$–EC/DEC/EMC, the price of inhibiting Al foil corrosion is sacrificing the excellent ionic conductivity of the LiFSI-based electrolyte. In order to minimize the cost, it is necessary to study additional amounts of the LiBOB and adjusting the solvent ratio. Besides, it remains a significant challenge to understand the relationship between the optimal proportions of salts and solvents as well as the effect on the performance of batteries. Obviously, the traditional orthogonal test method cannot meet the requirement.[18] Also, it is not practical to evaluate the electrolyte performance by cycle performance, rate performance and storage performance indirectly for taking too long a time.

[a]*School of Petrochemical Technology, Lanzhou University of Technology, Lanzhou 730050, P. R. China. E-mail: lishiyoulw@163.com; Fax: +86-931-7823001; Tel: +86-931-7823125*

[b]*Gansu Engineering Laboratory of Electrolyte Material for Lithium-ion Battery, Lanzhou 730050, P. R. China*

[c]*School of Materials Science and Engineering, Linyi University, Linyi, Shandong 276005, P. R. China*

Table 1 The level table with five factors and six levels

	One	Two	Three	Four	Five
①	1	2	3	4	5
②	2	3	4	5	1
③	3	4	5	1	2
④	4	5	1	2	3
⑤	5	1	2	3	4
⑥	6	6	6	6	6

In this work, a method combining simplex optimization with electrochemical testing was proposed to optimize the electrolyte with five components (including a lithium salt and solvents) and obtain the desired results in a short time and an economical way. The excellent inhibition ability of the optimized electrolyte was further examined *via* X-ray photoelectron spectroscopy (XPS), analysis of Al foil corrosion and electrochemical impedance spectroscopy (EIS) measurements of $LiFePO_4$/Li half cells, illustrating the effectiveness of the method and explaining the mechanism of excellent performance.

2. Experimental

2.1 Preparation of electrolyte

Battery-grade ethylene carbonate (EC), ethyl methyl carbonate (EMC), and diethyl carbonate (DEC) were provided by Chaoyang Yongheng Chemical Co., Ltd. Battery-grade LiFSI and LiBOB were purchased from Huizhou Avenue New Materials Co., Ltd. The preparation was conducted in glove box under Ar atmosphere, and both of the contents of water and oxygen were less than 0.1 ppm.

The electrolyte is consisting of five components. According to the requirements of simplex method, the initial simplex list should be determined by a list of five factors and six levels. The designed five factors table is shown in Table 1, which is the basis of preparing six groups of the initial electrolyte of E01–E06 in the Table 2. The first six columns of Table 2 are the specific representation of Table 1. The electrolyte of 0.6 mol L^{-1} LiFSI + 0.4 mol L^{-1} LiBOB–EC/DEC/EMC (1 : 1 : 1) is optimized. Additionally, the composition of electrolytes is calculated and designed accordance with simplex method.[19–22]

2.2 Electrode and cell preparation

The battery-grade Al foils (20 μm thickness, >99.45% purity) were provided by Alnan Aluminium Co. Ltd., coin cell cases (EQ-CR2025-CASE button cells case), and the battery-grade lithium foil were kindly offered by Shenzhen Kejing Star Technology Ltd. The $LiFePO_4$ (Hunan Shanshan Advanced Materials Co. Ltd.) electrodes were prepared by mixing 80 wt% cathode materials, 10 wt% acetylene and 10 wt% polyvinylidene fluoride (PVDF). The mass loading of the cathode electrodes was about 2.0 mg cm^{-2}. Assembly of $LiFePO_4$/Li half cells was conducted in a glove box in an Ar atmosphere with water and oxygen content less than 0.1 ppm.

2.3 Measurements

The leakage current was measured in three electrode system with Al foil as the working electrode. To ensure the consistent condition, the Al foil covers the area of 1 cm × 1 cm, 20 μm of thickness, and the area of the Al foil immersed in electrolyte was 0.1 cm^2. The lithium pieces were selected as the reference electrode and the auxiliary electrode. The three-electrode system was placed in an incubator with 45 °C. After 30 minutes, constant potential of 4.2 V was applied to the three-electrode system, and the current change in the system was recorded within 6 hours. The test was carried out by the electrochemical workstation of CHI660E. The ionic conductivity of electrolyte was measured by conductivity meter at 25 °C. Electrochemical impedance spectroscopy (EIS) was performed over frequencies from 0.01 Hz to 100 kHz at 5 mV. The concentration of aluminium ion (Al^{3+}) was determined with inductively coupled plasma atomic emission spectrometry (ICP-AES, Leeman, USA). The surface morphologies of Al foils were characterized by scanning electron microscopy (SEM, JSM-6510, Japan). Electrochemical charge–discharge tests were carried out on a LAND battery tester at 0.5C.

3. Results and discussion

For electrochemical tests, it is relatively more convenient to evaluate electrolytes based on the basic parameters of electrolyte, including the excellent film-forming property, high ion conductivity and the inhibition ability against Al corrosion.[23–27] Compared with the battery test, the electrochemical tests for electrolyte are relatively simple and fast. Nonetheless, it is important to determine whether the results of electrochemical tests for electrolyte are consistent with the result of the battery test. If there are uniform result, the electrochemical tests for electrolyte can be used to optimize the electrolyte system rightly and quickly. Therefore, the optimization processes are as

Table 2 Electrolyte composition

Number	LiFSI (g)	LiBOB (g)	EC (mL)	DEC (mL)	EMC (mL)	C_{LiFSI} (mol L^{-1})	C_{LiBOB} (mol L^{-1})
E01	0.36	0.27	1.3	1.4	1.5	0.46	0.33
E02	0.38	0.29	1.4	1.5	1.1	0.51	0.37
E03	0.40	0.31	1.5	1.1	1.2	0.56	0.42
E04	0.42	0.33	1.1	1.2	1.3	0.62	0.47
E05	0.44	0.25	1.2	1.3	1.4	0.60	0.33
E06	0.46	0.35	1.6	1.6	1.6	0.39	0.38

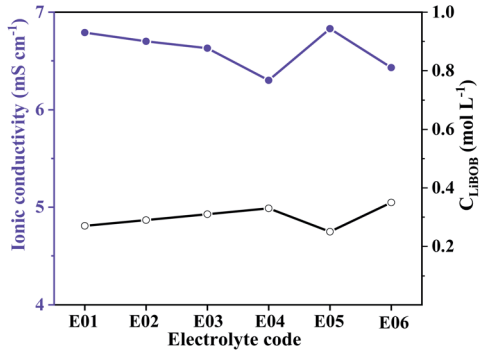

Fig. 1 Ionic conductivity for electrolytes with different concentration of LiBOB in the initial simplex at 25 °C.

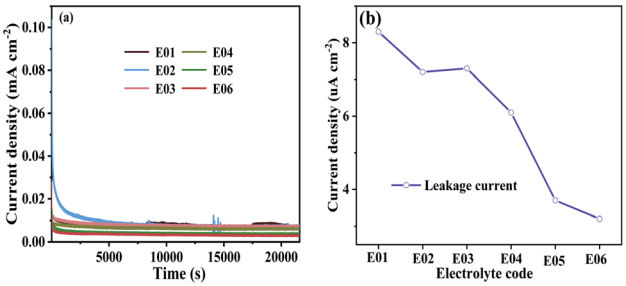

Fig. 2 (a) Chronoamperometry curves with the constant potential of 4.2 V for electrolytes in the initial simplex and Al as working electrodes, and (b) current value at the end of the chronoamperometry curves.

follows: seeking optimal index, normalizing the optimal index, optimization and verifying the results.

(1) Seeking optimal index. Firstly, to determine the electrochemical tests for electrolytes according to the basic parameters of electrolyte, one of the most basic parameters is excellent film-forming property. That is to say, the formed CEI film is stable and contributes to the transport of lithium ions.[28] The stability of CEI film is affected by its dielectric ability and the tendency against dissolving in electrolyte. The film-forming ability of electrolyte is evaluated by the test of leakage current at the interface. Secondly, the Al current collector passivated is another basic parameter. Al current collector is a key component of the cathode, and the electrochemical stability in the electrolyte directly determines the battery performance. The electrochemical stability of the Al collector in the electrolyte can also be tested by the leakage current.[29] Another basic parameter of electrolyte is the enough high ionic conductivity to facilitate the transport of lithium ions, which can be obtained by conductivity meter.

(2) Normalizing the optimal index. The index of optimization is normalized, and the normalized results are considered to score electrolytes. We can directly judge the quality of electrolytes according to the score of the electrolytes.

(3) Optimization. It is critical and intricate to determine and choose the ultimate optimization index. Once the optimization index is determined, the optimization of electrolyte becomes easy. Then, the electrolyte is prepared and the optimization parameters are determined until the optimization parameters coincides with the actual results.

(4) Verifying the results. The reliability of the optimized results is verified by the battery test.

3.1 Seeking optimal index

The electrolyte of $LiFSI_{0.6}$–$LiBOB_{0.4}$–EC/DEC/EMC (1 : 1 : 1) can be effectively used to suppress Al corrosion, because the robust and protective interphase are generated on Al current collector. In order to optimize the electrolyte, we seek the optimal index firstly. The ionic conductivity is one of the most basic parameters for electrolyte, the ionic conductivity of electrolytes based on the simplex method in Tables 1 and 2 was tested. Fig. 1 shows the ionic conductivity for six groups of electrolytes numbering from E01 to E06. It is quite obvious that the concentration of LiBOB salt plays a leading role in the ionic conductivity of electrolytes, the ionic conductivity of electrolytes decreases along with the increase of LiBOB salt concentration from number E01 to E04. The ionic conductivity of electrolyte lower, the rate performance worse. Therefore, it's necessary to decrease the concentration of LiBOB for electrolytes. Then the basic parameters of film-forming property for electrolytes on the Al foil will be analysed. The result for leakage current curves is shown in Fig. 2. The results show that the stability of CEI film obviously reduces with the concentration of LiBOB diminished. The amount of LiBOB in electrolyte is necessary to be increased so as to inhibit corrosion of Al current collector. The factors seem to contradict and constrain each other. Therefore, there must be an equilibrium point to determine the amount of LiBOB salt and LiFSI salt in the electrolyte.

The electrochemical and physicochemical tests for electrolyte have been completed, and the optimal index was analysed depending on whether the sorted result of cycle performance is

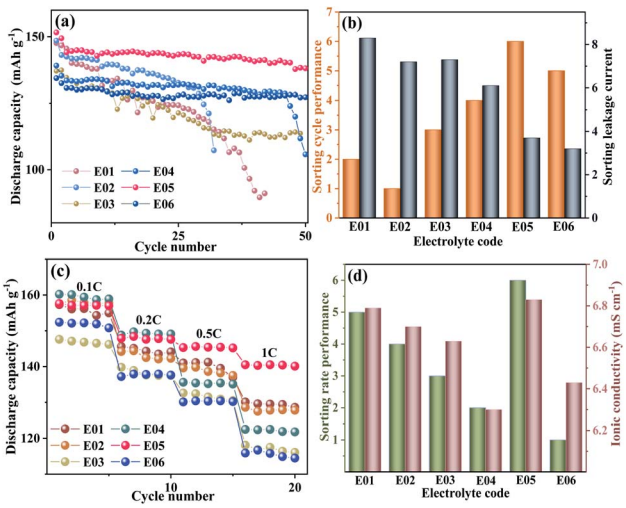

Fig. 3 The electrochemical properties electrolytes in the initial simplex: (a) cycle performance of $LiFePO_4$/Li half cells at 0.5C and 45 °C. (b) The sorting of cycle performance and leakage current. (c) Rate performance of $LiFePO_4$/Li half cells and (d) the sorting of rate performance and ionic conductivity.

consistent with the sorted result of the ionic conductivity or the stability of CEI film for electrolyte. Fig. 3a shows the cycle performance of $LiFePO_4$/Li half cells with six kinds of electrolytes, the cycle performance of E05 is the best in the six electrolytes. The six electrolytes were ranked by the cycle performance and the stability of CEI film, respectively, as shown in the Fig. 3b. As the value of the leakage current decreasing, the cycle performance of the battery improves. Namely, it shows that the sort of stability of CEI film is consistent with the cycle performance of the battery, which can be evaluated by the leakage current. However, the sort of the cycle performance of the batteries for the E06 electrolyte is abnormal in the trial. In theory, the electrolyte E06 with the lowest leakage current is supposed to have the best cycle performance. Compared with E05, the cycle performance of E06 is more stable and the discharge specific capacity is lower, hence the cycle performance of E06 is next to that of E05. It demonstrates that the cycle performance of battery is affected by the other properties of electrolyte. Although the leakage current of the electrolyte E06 is the lowest, E06 has the minimum concentration of LiFSI among the six electrolytes. The concentration of lithium ion (Li^+) in the electrolyte is 0.78 mol L^{-1}, the low specific discharge capacity is attributed to the lower content of Li^+ in the electrolyte. The results suggests that it is not accurate to evaluate electrolyte only by the leakage current. Therefore, it is necessary to combine other indicators for comprehensive evaluation. Fig. 3c shows the rate performance of battery with different electrolytes. The variation trend of rate performance is theoretically consistent with the ionic conductivity. The rate performance is visually displayed through the sort, which is based on the ratio of the arithmetic mean of the specific discharge capacity during 5 cycles at 1C to that in 5 cycles at 0.1C. The larger the ratio, the better the rate performance. The sorting results for rate performance and ionic conductivity are shown in Fig. 3d. It clearly shows that the rate performance is dependent upon ionic conductivity of electrolyte. Obviously, the sorting of rate performance is consistent with ionic conductivity for electrolytes apart from the group E06 with the lowest concentration of LiFSI. The finding suggests that ionic conductivity could also serve as the evaluation index of electrolyte. There is a discrepancy between what really happened and the results of evaluating electrolyte by leakage current or ionic conductivity alone. The comprehensive index of electrolyte evaluation can be obtained by combining ionic conductivity and leakage current.

In our previous work,[17] the corrosion mechanism of LiFSI-based electrolyte to Al current collector was studied at high temperature by adding LiBOB salt. It can be confirmed that in the electrolyte of $LiFSI_x$–$LiBOB_{(1-x)}$, the larger the amount of LiBOB salt is, the better the passivation effect of the electrolyte on Al current collector will be. But from the point of view of battery performance, excessive amount of LiBOB salt will result in the thickening of the CEI film, which caused many problems, for example, it decreases the coulombic efficiency, increases the internal impedance and polarization, and reduces the discharge capacity of the battery. Compared with optimization before, there is no significant difference in the amount of LiFSI and LiBOB, while the ratio of EC, DEC and EMC vary significantly. Therefore, the performance of electrolyte is different before and after optimization. That is largely because solvents have different effects on the corrosion of Al collector. Therefore, the effect of solvents on corrosion was studied. The electrolytes of 1 mol L^{-1} LiFSI/EC, 1 mol L^{-1} LiFSI/DEC and 1 mol L^{-1} LiFSI/EMC were tested by cyclic voltammograms. The results are shown in Fig. 4.

The different solvents do have different effects on the corrosion process of Al foil. The first anodic scan was processed with the potential growing even after the scanning direction is reversed at 5.0 V (Fig. 4a). After reaching the maximum, the anodic current decreases rapidly and nears zero at around 3.8 V. This counter-clockwise CV shape manifests severe Al corrosion behavior.[30–33] The Al foil is quite badly corroded in the electrolyte with EC, while the corrosion degree of Al foil in 1 mol L^{-1} LiFSI/DEC and 1 mol L^{-1} LiFSI/EMC are relatively weak. The phenomenon is related to the structure of three solvent molecules: EC with cyclic structure as well as DEC and EMC with linear structures. The lone electron pairs in three solvents play key roles in the solvation of Li^+ ions. The cyclic molecular structure of the cyclic EC is compact and small, and it has strong solvation ability for metal ions. Besides, the dielectric constant and polarity of EC is higher than DEC and EMC. Therefore, the Al foil is quite badly corroded in electrolyte with EC.

In order to determine whether the corrosion curves in Fig. 4 actually caused by the dissolution of corrosion products by solvent, the concentration of Al^{3+} in electrolyte was measured by ICP measurement after the cyclic voltammetry (CV) test. The results are shown in Table 3. The results showed that the concentrations of aluminium ion (Al^{3+}) in EC, DEC and EMC based electrolytes were 306.8 mg L^{-1}, 196.7 mg L^{-1} and 273.7 mg L^{-1}, respectively.

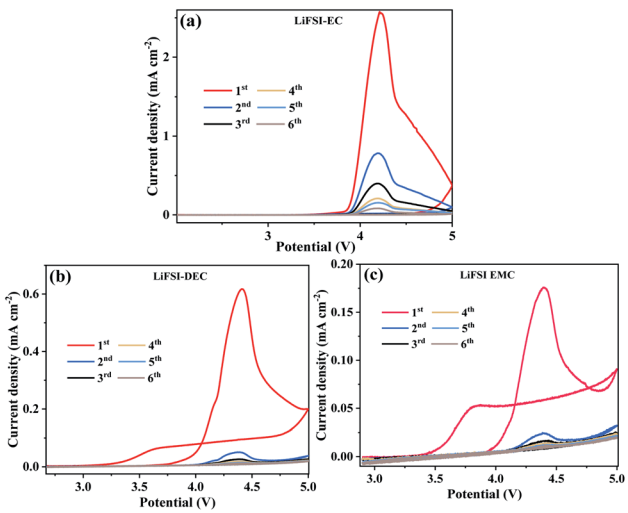

Fig. 4 First six cyclic-voltammetry curves of Al foil polarized in 1 mol L^{-1} LiFSI/EC (a), 1 mol L^{-1} LiFSI/DEC (b) and 1 mol L^{-1} LiFSI/EMC (c), respectively. Scanning started from OCP in the cathodic direction with a sweeping rate of 5 mV s^{-1} at 45 °C.

Table 3 Concentration of Al^{3+} in the electrolyte in the electrolytic cell after CV tests

Electrolyte	1 mol L^{-1} LiFSI/EC	1 mol L^{-1} LiFSI/DEC	1 mol L^{-1} LiFSI/EMC
Concentration of Al^{3+} (mg L^{-1})	306.8	196.7	213.7

Table 4 Score of electrolytes E01 to E09

	E01	E02	E03	E04	E05	E06	E07	E08	E09
σii	6.79	6.70	6.63	6.30	6.83	6.43	6.81	6.78	6.82
Iii	8.31	7.20	7.32	6.10	3.71	3.21	8.40	6.54	3.36
Ki	0.92	0.72	0.62	0	1	0.24	0.96	0.91	0.98
Li	0	0.22	0.2	0.43	0.9	1	−0.02	0.35	0.97
Sii	0.92	0.97	0.82	0.43	1.9	1.24	0.94	1.26	1.95

The concentration of Al^{3+} in EC-based electrolyte is the highest, it shows that the Al foil is quite badly corroded in the electrolyte with EC. The deposition layer on the surface of Al foil is serious destroyed by EC. That is to say, the solvent with high dielectric constant is not conducive to the stability of Al collector.

3.2 Normalizing the optimal index

In order to have a quantitative description for the performance of electrolyte during optimization process, the electrolyte index for ion conductivity and leakage current are needed to be dimensionless treatment. The treatment method is as follows.

For ionic conductivity, the Ki value of each electrolyte is

$$K[i] = \frac{\sigma[i] - \sigma min}{\sigma max - \sigma min}$$

σi (i = E01, E02, …) is the ionic conductivity of each electrolyte; σmin is the minimum value of ionic conductivity in the initial electrolyte, σmin = σE04. σmax is the maximum value of ionic conductivity in the initial electrolyte, σmax = σE05.

For the leakage current, the leakage current Li of each electrolyte is

$$L[i] = \frac{Imax - I[i]}{Imax - Imin}$$

Li (i = E01, E02, …) represents leakage current of each electrolyte, Imin is the minimum value of the leakage current of electrolytes in the initial simplex, its value Imin = IE06. Imax is the maximum value of the leakage current of the initial electrolyte, its value Imax = IE01. Then the comprehensive Si of the electrolyte is

$$Si = Ki + Li$$

After above-mentioned treatment, the Si of the initial electrolytes E01–E06 must have a minimum value, and the electrolyte with the minimum value is used as a reference point to find new electrolyte. The cut-off condition of the search process is to find a test point that with the Si value is maximum value, the search method is carried out according to simplex method. Table 4 shows the comprehensive scores of each group, including the three test points generated in the process of finding the maximum value of Si.

Table 4 shows that E05 group has the highest comprehensive score among the six groups for E01–E06 in the initial simplex optimal. These results are consistent with the sorting results of cycle performance and rate performance. It suggests that normalized for the optimization index is feasible. After three times of simplex optimization, as is shown in Table 5. We can obtain the possible maximum SE09 = 1.95. The composition of the E09 electrolyte is 0.53 mol L^{-1} LiFSI + 0.35 mol L^{-1} LiBOB–EC/DEC/EMC (1.3 : 1.5 : 1.5), denoted as $LiFSI_{0.53}$–$LiBOB_{0.35}$–EC/DEC/EMC (1.3 : 1.5 : 1.5). The E09 electrolyte is optimal.

3.3 Electrochemical performance test and mechanism analysis

Cycle performance of $LiFePO_4$/Li half-cells with $LiPF_6$-based electrolyte, unoptimized and optimized electrolyte at 45 °C is shown in Fig. 5a. The specific discharge capacity of unoptimized and optimized electrolyte after 100 cycles is 133.8 mA h g^{-1} and 143.1 mA h g^{-1}, respectively, and the capacity retention rate is 90.28% and 94.89%, respectively. The cycle stability and the specific discharge capacity are also improved in the optimized electrolyte, compared with commercial $LiPF_6$–EC/DEC electrolyte. Obviously, $LiPF_6$-based electrolyte is not suitable for high temperature. Fig. 5b shows the rate performance of $LiFePO_4$/Li half cells for the three electrolytes. The rate performance of the optimized electrolyte

Table 5 Electrolyte composition

Number	LiFSI (g)	LiBOB (g)	EC (mL)	DEC (mL)	EMC (mL)	C_{LiFSI} (mol L^{-1})	C_{LiBOB} (mol L^{-1})
E07	0.40	0.28	1.6	1.5	1.4	0.48	0.3
E08	0.41	0.31	1.3	1.3	1.3	0.57	0.41
E09	0.42	0.29	1.3	1.5	1.5	0.53	0.35

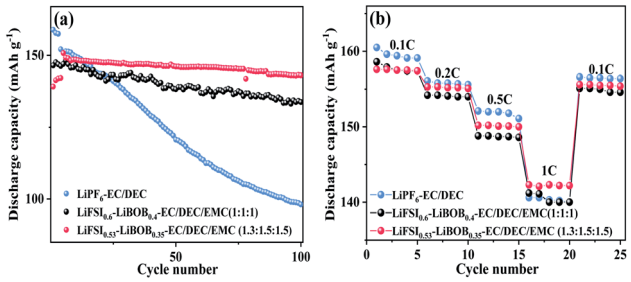

Fig. 5 Cycle performance (a) and rate performance data (b) of $LiFePO_4$/Li half-cells with $LiPF_6$-based electrolyte, unoptimized electrolyte and optimized electrolyte at 45 °C.

is inferior to $LiPF_6$–EC/DEC electrolyte, the performance at high-rate of the optimized electrolyte at 1C is better than $LiPF_6$–EC/DEC electrolyte. The optimized electrolyte $LiFSI_{0.53}$–$LiBOB_{0.35}$–EC/DEC/EMC (1.3 : 1.5 : 1.5) has the lower ionic conductivity, and the excellent CEI film constructed on the electrode surface for the optimized electrolyte makes the battery show the optimal rate performance at high-rate and cycle performance. The results show that the optimized electrolyte has the best performance, which shows that the optimized result is reliable.

We also analysed the corrosion inhibition of Al foil by electrolytes by disassembling the battery after cycling and carefully scraping off the material on the surface of electrode. The surface morphology of Al current collector is shown in Fig. 6. The fragments of electrode materials make no difference to the observation of the surface morphology. The surface of Al collector is flat without corrosion pit and crack in Fig. 6a, the contact between the electrode material and the Al collector is well without peeling (Fig. 6b). The phenomenon makes abundantly clear that the Al current collector is stable in the optimized electrolyte. There are small holes in Fig. 6c and there are shallow pits on the flat surface of the substrate in Fig. 6d, which is the result of hydrogen fluoride (HF) corrosion to Al current collector produced by decomposition of $LiPF_6$.

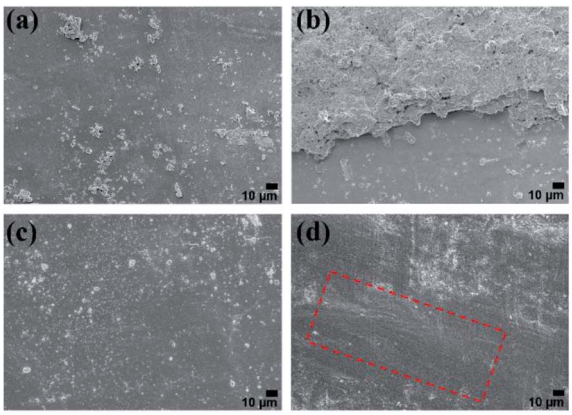

Fig. 6 SEM images of Al current collector surface for the $LiFePO_4$/Li battery without cycling (a), after cycle with optimized electrolyte (b), unoptimized electrolyte (c) and $LiPF_6$-based electrolyte (d).

The surface composition of Al current collector after cycle was characterized by XPS in the electrolyte before and after optimization, as is shown in Fig. 7. The F 1s spectrum (Fig. 7a1) shows two major peaks at 685.0 and 686.6 eV, confirming the presence of lithium fluoride (LiF) and aluminium fluoride (AlF_3) on the surface of the Al foil. In addition, the minor peak located at 687.7 eV corresponds to $Al(FSI)_3$.[34,35] The B–O peak at 191.8 eV in the B 1s spectrum comes from the compound in the passive film containing B–O bond.[36–38] The passivation film of Al collector was formed in the optimized electrolyte, and the decomposition products of LiBOB and LiFSI include boron trioxide (B_2O_3), LiF and AlF_3. However, the decomposition products are mainly LiF and compounds containing B–O bond in the unoptimized electrolyte. Our previous research shows that the main corrosion products of Al foil in LiFSI based electrolyte are AlF_3 and $Al(FSI)_3$ at 45 °C. The reason for the formation of a large amount of $Al(FSI)_3$ is the porosity of AlF_3 and the continuous dissolution of Al foil. Compared with the unoptimized electrolyte, the proportion of $Al(FSI)_3$ in the passivation film is low in the optimized electrolyte. It suggests that the compact AlF_3 is formed, and the stability of Al current collector is increased. It indicates that AlF_3 can inhibit corrosion. Additionally, the contents of AlF_3 and B_2O_3 in the passivation film are increased in the optimized electrolyte. Compared with Fig. 7c1 and c2, it can be concluded that the proportion of solvent in the electrolyte does affect the formation of passivation film on the surface of Al current collector. Obviously, the content of lithium carbonate (Li_2CO_3) in the passivation film formed in optimized electrolyte is increased, which improves the firmness of the passivation film.[39–41]

To further analyze the effect electrolyte on battery, Nyquist plot (Fig. 8) was recorded after 100 cycles. The cell with the optimized electrolyte has a smaller interface impedance, which further shows that the CEI film formed on the electrode surface is stable and is beneficial to transportation of lithium ions. However, the interface impedance of $LiPF_6$–EC/DEC electrolyte is the largest, which indicates that the film formed by $LiPF_6$ electrolyte at 45 °C has poor lithium conductivity, which is not conducive to large rate charge and discharge. This is also the reason why the optimized electrolyte the rate performance is superior to $LiPF_6$ electrolyte in 1C cycle.

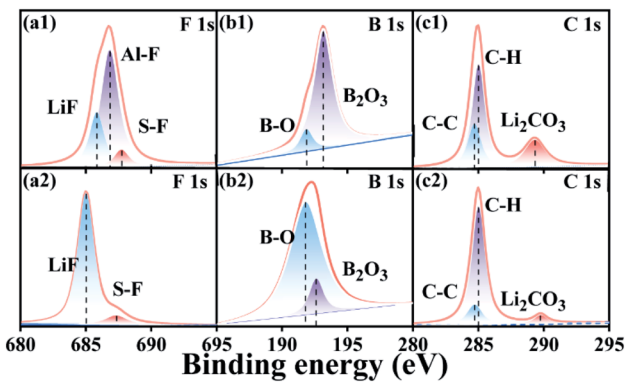

Fig. 7 XPS spectra of the Al current collectors after cycle with the optimized (a1, b1, c1) and unoptimized (a2, b2, c2) electrolyte.

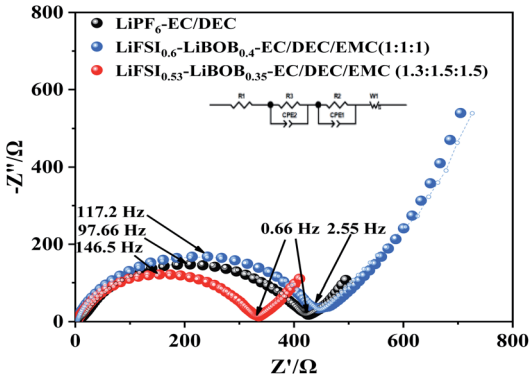

Fig. 8 Nyquist plots of cycled $LiFePO_4$/Li half-cells with optimized electrolyte, unoptimized electrolyte and $LiPF_6$-based electrolyte.

4. Conclusions

We systematically optimized electrolyte $LiFSI_{0.6}$–$LiBOB_{0.4}$–EC/DEC/EMC (1 : 1 : 1) by combining the method of simplex with normalization. Among the electrolytes, the capacity of the $LiFePO_4$/Li half-cell with the optimized electrolyte $LiFSI_{0.53}$–$LiBOB_{0.35}$–EC/DEC/EMC (1.3 : 1.5 : 1.5) displays a high capacity of 143.1 mA h g^{-1} after 100 cycles at 0.5C at 45 °C with the capacity retention of 94.9%. The optimized electrolyte was revealed to be an excellent Al corrosion inhibitor through CV and SEM experiments. The mechanism of the improvement of battery performance by salts and solvents in the electrolyte studies indicates that the increase contents of LiFSI and LiBOB salts is helpful to improve the ionic conductivity of electrolyte and the stability of CEI film, respectively. In addition, with the solvent of EC content increasing, the dissolution of surface film on Al current collector intensifies. The XPS analysis reveals that the solid and dense LiF, AlF_3, B_2O_3 and Li_2CO_3 in the passivation film on Al current collector contribute to the superior inhibition ability against Al corrosion. This study puts forward a promising strategy to optimize LiFSI-based electrolytes to alleviate Al corrosion.

Conflicts of interest

There are no conflicts to declare.

Acknowledgements

This work was supported by the Natural Science Foundation of China (21766017 and 51962019), the Natural Science Foundation of Qinghai Province of China for Youth Project (2019-ZJ-938Q), Shandong Provincial Natural Science Foundation Project (ZR2020MB082) and Lanzhou University of Technology Hongliu First-class Discipline Construction Program.

References

1 Z. Wang, A. Hofmann and T. Hanemann, *Electrochim. Acta*, 2019, **298**, 960–972.
2 S. Liu, Q. Zhang, X. Wang, M. Xu, W. Li and B. L. Lucht, *Appl. Surf. Sci.*, 2020, **12**, 33719–33728.
3 H. Zhang, C. Shen, Y. Huang and Z. Liu, *Appl. Surf. Sci.*, 2021, **537**, 147983.
4 S. Klein, S. van Wickeren, S. Roser, P. Barmann, K. Borzutzki, B. Heidrich, M. Borner, M. Winter, T. Placke and J. Kasnatscheew, *Adv. Energy Mater.*, 2021, **11**, 2003738.
5 K. Xu, *Chem. Rev.*, 2004, **104**, 4303–4417.
6 F. N. Sayed, M. T. F. Rodrigues, K. Kalaga, H. Gullapalli and P. M. Ajayan, *Appl. Surf. Sci.*, 2017, **9**, 43623–43631.
7 E. Markevich, G. Salitra and D. Aurbach, *ACS Energy Lett.*, 2017, **2**, 1337–1345.
8 D. Zhao, J. Wang, P. Wang, H. Liu and S. Li, *Electrochim. Acta*, 2020, **337**, 135745.
9 M. Kerner, N. Plylahan, J. Scheers and P. Johansson, *RSC Adv.*, 2016, **6**, 23327–23334.
10 S. Das, *J. Electroanal. Chem.*, 2020, **879**, 114794.
11 A. Wei, W. Li, Q. Chang, X. Bai, R. He, L. Zhang, Z. Liu and Y. Wang, *Electrochim. Acta*, 2019, **323**, 134692.
12 L. Suo, W. Xue, M. Gobet, S. G. Greenbaum, C. Wang, Y. Chen, W. Yang, Y. Li and J. Li, *Proc. Natl. Acad. Sci. U. S. A.*, 2018, **115**, 1156–1161.
13 H. Zhou, K. Xiao and J. Li, *J. Power Sources*, 2016, **302**, 274–282.
14 H. Zhou, D. Xiao, C. Yin, Z. Yang, K. Xiao and J. Li, *J. Electroanal. Chem.*, 2018, **808**, 293–302.
15 L. Zhang, L. Chai, L. Zhang, M. Shen, X. Zhang, V. S. Battaglia, T. Stephenson and H. Zheng, *Electrochim. Acta*, 2014, **127**, 39–44.
16 K. Xu, *Chem. Rev.*, 2014, **114**, 11503–11618.
17 C. L. Li, S. W. Zeng, P. Wang, Z. J. Li, L. Yang, D. N. Zhao, J. Wang, H. N. Liu and S. Y. Li, *Trans. Nonferrous Met. Soc. China*, 2021, **31**, 1439–1451.
18 Y. Yamada, C. H. Chiang, K. Sodeyama, J. Wang, Y. Tateyama and A. Yamada, *ChemElectroChem*, 2015, **2**, 1687–1694.
19 I. A. Shkrob, K. Z. Pupek and D. P. Abraham, *J. Phys. Chem. C*, 2016, **120**, 18435–18444.
20 F. Ahmed, M. M. Rahman, S. C. Sutradhar, N. S. Lopa, T. Ryu, S. Yoon, I. Choi, Y. Lee and W. Kim, *Electrochim. Acta*, 2019, **302**, 161–168.
21 J. Liu, X. Song, L. Zhou, S. Wang, W. Song, W. Liu, H. Long, L. Zhou, H. Wu, C. Feng and Z. Guo, *Nano Energy*, 2018, **46**, 404–414.
22 Y. Zhu, X. Luo, M. Xu, L. Zhang, L. Yu, W. Fan and W. Li, *J. Power Sources*, 2016, **317**, 65–73.
23 S. Dutta, S. Pal and S. De, *New J. Chem.*, 2019, **43**, 12385–12395.
24 X. Cao, L. Zou, B. E. Matthews, L. Zhang, X. He, X. Ren, M. H. Engelhard, S. D. Burton, P. Z. El-Khoury, H. S. Lim, C. Niu, H. Lee, C. Wang, B. W. Arey, C. Wang, J. Xiao, J. Liu, W. Xu and J. G. Zhang, *Energy Storage Materials*, 2021, **34**, 76–84.
25 Q. Xu, T. Chen, Z. Wu, Y. Liu, L. Qiu, Z. Yang, D. Wang, W. Xiang, B. Zhong and X. Guo, *Ind. Eng. Chem. Res.*, 2020, **59**, 1568–1577.
26 D. Y. Wang, A. Xiao, L. Wells and J. R. Dahn, *J. Electrochem. Soc.*, 2015, **162**, A169–A175.

27 F. Huang, G. Ma, Z. Wen, J. Jin, S. Xu and J. Zhang, *J. Mater. Chem. A*, 2018, **6**, 1612–1620.
28 J. Wang, Y. Yamada, K. Sodeyama, C. H. Chiang, Y. Tateyama and A. Yamada, *Nat. Commun.*, 2016, **7**, 12032.
29 G. Ma, L. Wang, X. He, J. Zhang, H. Chen, W. Xu and Y. Ding, *ACS Appl. Energy Mater.*, 2018, **1**, 5446–5452.
30 M. Morita, T. Shibata, N. Yoshimoto and M. Ishikawa, *Electrochim. Acta*, 2002, **47**, 2787–2793.
31 L. Li, S. Zhou, H. Han, H. Li, J. Nie, M. Armand, Z. Zhou and X. Huang, *J. Electrochem. Soc.*, 2011, **158**, A74–A82.
32 K. Park, S. Yu, C. Lee and H. Lee, *J. Power Sources*, 2015, **296**, 197–203.
33 S. Kaya, P. Banerjee, S. K. Saha, B. Tüzün and C. Kaya, *RSC Adv.*, 2016, **6**, 74550–74559.
34 J. Zheng, X. Fan, G. Ji, H. Wang, S. Hou, K. C. DeMella, S. R. Raghavan, J. Wang, K. Xu and C. Wang, *Nano Energy*, 2018, **50**, 431–440.
35 S. J. Kang, K. Park, S. H. Park and H. Lee, *Electrochim. Acta*, 2018, **259**, 949–954.
36 X. Luo, *J. Alloys Compd.*, 2018, **730**, 23–30.
37 A. Mauger, C. M. Julien, A. Paolella, M. Armand and K. Zaghib, *Mater. Sci. Eng., R*, 2018, **134**, 1–21.
38 L. Xia, Y. Jiang, Y. Pan, S. Li, J. Wang, Y. He, Y. Xia, Z. Liu and G. Z. Chen, *ChemistrySelect*, 2018, **3**, 1954–1960.
39 S. Huang, S. Wang, G. Hu, L. Z. Cheong and C. Shen, *Appl. Surf. Sci.*, 2018, **441**, 265–271.
40 J. Lochala, T. Taverne, B. B. Wu, M. Benamara, M. Cai, X. C. Xiao and J. Xiao, *Nano Lett.*, 2016, **16**, 2011–2016.
41 G. Wen, L. Tan, X. X. Lan, H. Y. Zhang, R. Z. Hu, B. Yuan, J. Liu and M. Zhu, *Sci. China Mater.*, 2021, DOI: 10.1007/s40843-021-1665-1.